# Biological Synthesis of Gold Nanowires Using Extract of *Rhodopseudomonas capsulata*

**Shiying He, Yu Zhang, Zhirui Guo, and Ning Gu***

State Key Laboratory of Bioelectronics and Jiangsu Laboratory for Biomaterials and Devices, Southeast University, Nanjing, 210096, P. R. China

An environmentally friendly method using a cell-free extract (CFE) of *Rhodopseudomonas capsulata* is proposed to synthesize gold nanowires with a network structure. This procedure offers control over the shapes of gold nanoparticles with the change of $HAuCl_4$ concentration. The CFE solutions were added with different concentrations of $HAuCl_4$, resulting in the bioreduction of gold ions and biosynthesis of morphologies of gold nanostructures. It is probable that proteins acted as the major biomolecules involved in the bioreduction and synthesis of gold nanoparticles. At a lower concentration of gold ions, exclusively spherical gold nanoparticles with sizes ranging from 10 to 20 nm were produced, whereas gold nanowires with a network structure formed at the higher concentration of gold ions in the aqueous solution. This method is expected to be applicable to the synthesis of other metallic nanowires such as silver and platinum, and even other anisotropic metal nanostructures are expected using the biosynthetic methods.

## Introduction

The current interest in nanomaterials is focused on the controllable properties of size and shape because the optical, electronic, magnetic, and catalytic properties of metal nanoparticles strongly depend on their sizes (*1*) and shapes (*2*, *3*). The remarkable different optical properties of gold nanorods and nanotriangles are some examples of exciting shape-dependent properties, in which gold nanorods show two absorption peaks arising from the transverse and longitudinal surface plasmon resonances (SPR), whereas the spherical shapes display only a single SPR peak (*4*). Nanocubes (*5*), nanorods (*6*), nanowires (*7*, *8*), nanoplates (*9*), nanobelts (*10*), and nanotadpoles (*11*) can be synthesized by conventional chemical and physical methods. The majority of the current chemical production processes are regarded as having a relatively high environmental cost. There is increasing pressure to develop clean, nontoxic, and environmentally benign synthetic technologies. Recently biosynthetic methods employing either microorganism (*12*) or plant extracts have emerged as environmentally sustainable alternatives to chemical synthetic procedures. An earlier study found that *Bacillus subtlis* 168 was able to reduce $Au^{3+}$ ions to gold nanoparticle with a range of 5−25 nm inside the cell walls (*13*). Recently, Sastry and co-workers reported some biological syntheses of gold and silver nanoparticles using microorganisms intracellularly (*14*, *15*) or extracellularly (*16*, *17*). The shape-selective formation of single crystalline triangular gold nanoparticles was observed using extracts of lemongrass (*18*) and aloe vera (*19*) plants. Xie and co-workers (*20*) reported synthesis gold nanoplates in an extract of algal and identified that proteins acted as the primary reducing and shape-directing agent.

However, the biosynthesis of gold nanowires using microorganisms or plant extracts has been rarely reported. The availability of nanowires in large quantity would be of great importance in microelectronics, optoelectronics, nanoscale electronic devices, and other fields. In this study, we report on the simple biological synthesis of networked nanowires by the reaction of aqueous chloroaurate ions with an extract of *Rhodopseudomonas capsulata* at room temperature. *R. capsulata*, recognized as an ecologically and environmentally important microorganism, has been used for the treatment of pollution. It contains about 65% proteins, 20% soluble polysaccharide, 7% lipids, 3% fibers, bacteriochlorophyll, and vitamins. Biomolecules with carboxyl, hydroxyl, and amine functional groups have the potential for metal-ion reduction and for capping the newly formed nanoparticles (*21*). In previous work, it was found that the bacterium could be used to reduce Au(III) to Au(0) extracellularly (*22*). The morphology of gold nanoparticles synthesized using CFE could be modulated by the concentration of gold ions. At a lower concentration of gold ions, exclusively spherical gold nanoparticles were produced, whereas gold nanowires with a networked structure formed at a higher concentration of gold ions in the aqueous solution.

## Experiment Section

**Materials.** All chemical agent including chloroauric acid ($HAuCl_4$), purvate, yeast extract, NaCl, $NH_4Cl$, and $K_2HPO_4$ were obtained from Shanghai Chemical Reagent Co. Ltd. and used as received.

**Microorganisms and Culture Conditions.** The mixed culture of *R. capsulata* was cultured in a medium containing pyruvate, yeast extract, NaCl, $NH_4Cl$, and $K_2HPO_4$ at pH 7 and 30 °C. After 96 h of fermentation, the cells were separated from the culture broth by centrifugation (5000 rpm) at 10 °C for 10 min and washed five times with deionized water (18.2 $M\Omega cm^{-1}$) to obtain about 1 g wet weight of cells.

**Cell-Free Extract Preparation.** The harvested cells were then resuspended in 10 mL of deionized water for 15 days. The cells were then removed by centrifugation, and the aqueous supernatant obtained was cell-free extract (CFE).

* To whom correspondence should be addressed. Fax: (+86) 25-8379-4960. Tel: (+86) 25-8379-2576. E-mail: guning@seu.edu.cn.

10.1021/bp0703174 CCC: $40.75 © 2008 American Chemical Society and American Institute of Chemical Engineers
Published on Web 02/23/2008

**Synthesis of Gold Nanoparticles.** The CFE solution thus prepared was a light yellow liquid and was used for the reduction of $HAuCl_4$. To test tubes containing 10 mL of CFE solution was added 50−100 $\mu$L of 0.05 M aqueous $HAuCl_4$ solution. All experiments were conducted at 30 °C and pH 6 for 48 h, during which time reduction of $Au^{3+}$ in all of the reaction mixtures had occurred. The products were characterized by UV−vis NIR spectroscopy, transmission electron microscopy (TEM), and Fourier transform infrared (FTIR) spectroscopy analysis.

**UV−vis NIR Absorbance Spectroscopy Studies**. The UV−vis spectra for the reaction solution of gold nanoparticles were measured on a Shimadzu spectrophotometer (model UV-3150PC) operated at a resolution of 1 nm.

**TEM Measurements.** TEM samples of the gold nanoparticles synthesized using the CFE were prepared by placing 5 $\mu$L of the product solution onto carbon-coated copper grids and allowing the solvent to evaporate in the air. TEM measurements were performed on a JEOL, model JEM-200EX instrument operated at an accelerating voltage of 120 kV.

**FTIR Measurements.** For FTIR spectrum analysis, the gold nanoparticles synthesized using the CFE were centrifuged at 10 000 rpm for 20 min to remove free proteins or other compounds present in the solution. The centrifuged, collected, and vacuum-dried particles were made in a KBr pellet and the spectrum was recorded with a Nicolet Magna FTIR-750 spectrometer.

**EDX Measurements.** The chemical composition of the products was determined by energy-dispersive X-ray spectroscopy (EDX) using an INCA energy spectrometer (Oxford instrument, Britain).

**Sodium Dodecylsulfate Polyacrylamise Gel Electrophoresis (SDS-PAGE) Analysis.** SDS-PAGE was used to identify the numbers of proteins and their molecular weight in the CFE. The harvested cells after 96 h of growth were resuspended in 10 mL of the deionized water for 15 days. The cells were then removed by centrifugation, and the aqueous supernatant was concentrated by ultrafiltration (molecular weight cutoff = 8 k) and then dialyzed thoroughly against distilled water using a 8 k cutoff dialysis bag. This concentrated aqueous extract containing proteins was analyzed by SDS-PAGE.

**ICP Measurements.** The synthesized gold nanoparticles were removed by centrifugation and the soluble Au(III) ion concentration was measured using an inductively coupled plasma (ICP) Spectrometer (Thermo, USA).

## Results and Discussion

The primary variable in the reaction condition was the concentration of $HAuCl_4$ for different sets of samples. As is clear from the inset in Figure 1, the color changed from pale yellow to a vivid ruby red after 48 h of aging in the first reaction, where the concentration of $HAuCl_4$ was $2.5 \times 10^{-4}$ M. Such a color transition indicated the change in the metal oxidation and formation of gold nanoparticles. As shown in the Figure 1, UV−vis spectra recorded from this solution showed the appearance of a single but strong SPR band absorption peak centered at about 530 nm, which indicates that these particles are isotropic in shape and uniform in size.

Figure 2A shows the representative TEM images of the nanoparticles synthesized using CFE. TEM measurements revealed that at the lower initial concentration of $HAuCl_4$ ($2.5 \times 10^{-4}$ M) the gold nanoparticles formed were exclusively spherical with particle size ranging from 10 to 20 nm. This is consistent with the observed optical absorption spectrum. Figure

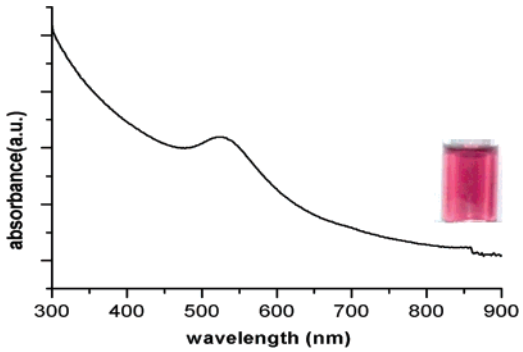


**Figure 1.** UV−visible spectra of gold nanoparticles prepared by CFE at $2.5 \times 10^{-4}$ M $HAuCl_4$. The inset shows the test tube of gold nanoparticles solution formed at the end of the reaction.

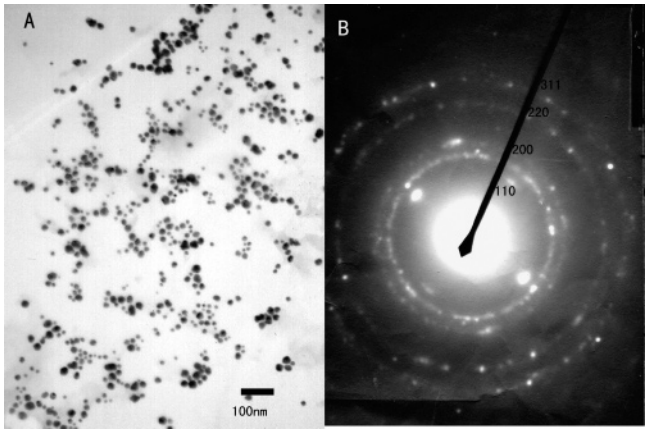


**Figure 2.** (A) Representative TEM image of gold nanoparticles produced by CFE at $2.5 \times 10^{-4}$ M $HAuCl_4$. (B) SAED pattern from gold nanoparticles corresponding to A.

2B shows the selected area electron diffraction (SAED) pattern obtained from the gold nanoparticles shown in Figure 2A. The Scherrer ring pattern characteristic of face-centered cubic (fcc) gold is clearly observed.

It was observed that the gold nanoparticles solution was extremely stable for at least 3 months with only little aggregation of particles in solution. The particles were stabilized in the solution by the capping agent, which is likely to be proteins secreted by the bacteria in the CFE. FTIR spectroscopy measurements were carried out to identify the biomolecules that bound specially on the gold surface. Figure 3A shows the presence of three bands at 1640, 1540, and 1450 $cm^{-1}$. The strong absorptions at 1640 and 1540 $cm^{-1}$ are characteristic of amide I and II bands (*23*) (labeled in Figure 3A) respectively. The amide band I is assigned to the stretch mode of the carbonyl group coupled to the amide linkage, while the amide II band arises as a result of the N−H stretching modes of vibration in the amide linkage. The band at approximately 1450 $cm^{-1}$ is assigned to the methylene scissoring vibrations from the proteins. The positions of these bands are close to earlier reports (*15*, *16*, *24*), indicating that the secondary structure of the enzyme is maintained on the gold surface. It is well-known that proteins can bind to gold nanoparticles through either free amine groups or cystein residues in the proteins (*24*) and therefore stabilization of the gold nanoparticles by the surface-bound proteins is possible. A spot profile EDAX spectrum recorded from the gold nanoparticles (Figure 3B) shows the presence of strong signals from the gold atoms together with weaker signals from C, O, N, and S atoms that arise from proteins bound to the gold nanoparticles. The presence of proteins in the CFE was also confirmed by SDS-PAGE analysis. Figure 3C shows

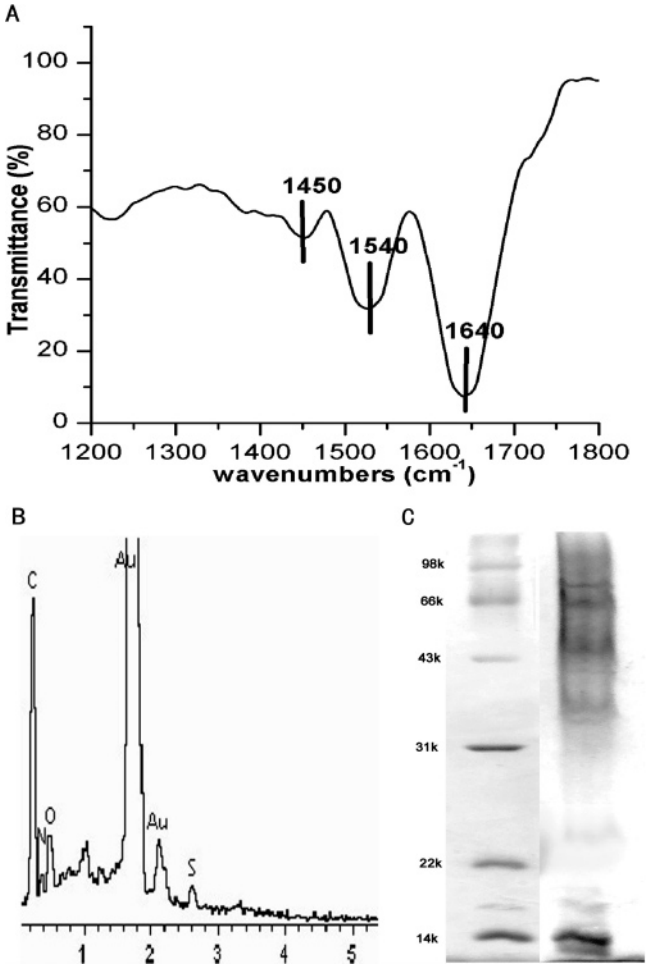


**Figure 3.** (A) FTIR spectrum of gold nanoparticles synthesized in the CFE. (B) Spot profile EDAX spectrum recorded from gold nanoparticles synthesized in the CFE. (C) SDS-PAGE analysis showing the proteins in the CFE. Lane 1 shows the standard protein molecular-weight markers with molecular weights given in kilodaltons. Lane 2 shows the proteins in the CFE and their approximate molecular weights.

that at least five different proteins of molecular masses between 14 and 98 kDa exist in the CFE. One or more of these proteins may be enzymes that reduce chloroaurate ions and cap the gold nanoparticles formed by the reduction process.

The high concentration of CFE relative to gold ions could result in a fast reduction, which exerts thermodynamic control in both nucleation and growth and thus leads to the final spherical nanostructures, regardless of the capping function of proteins in the CFE. As the concentration of $HAuCl_4$ was gradually increased, the shapes of the gold nanoparticles changed obviously. It was found that at the concentration of $3.0 \times 10^{-4}$ M $HAuCl_4$, larger nanoparticles formed. When the $HAuCl_4$ concentration was $4.0 \times 10^{-4}$ M, the color changed to blue during the reaction and turned red at the end of the reaction. The final product was spherical nanoparticles with a diameter between 20 and 30 nm and nanowires formed as middle product (Figure S1, Supporting Information).

When the concentration of $HAuCl_4$ solution was $5 \times 10^{-4}$ M, the reaction solution turned gray blue color as seen from the inset in Figure 4. Figure 4 shows the UV−vis absorption spectrum taken from the solution of gold nanowires. It should be noted that almost-flat absorbance curve with a board peak were observed from 500 to 900 nm. The flat adsorption pattern corresponded to the blue suspended solution in the reaction. The broad spectrum could be ascribed to the overlay of the

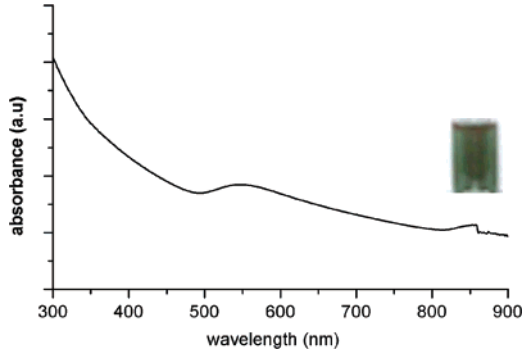


**Figure 4.** UV−visible spectra of gold nanowiress prepared by CFE at $5.0 \times 10^{-4}$ M $HAuCl_4$. The inset shows the test tube of gold nanowires solution formed at the end of the reaction.

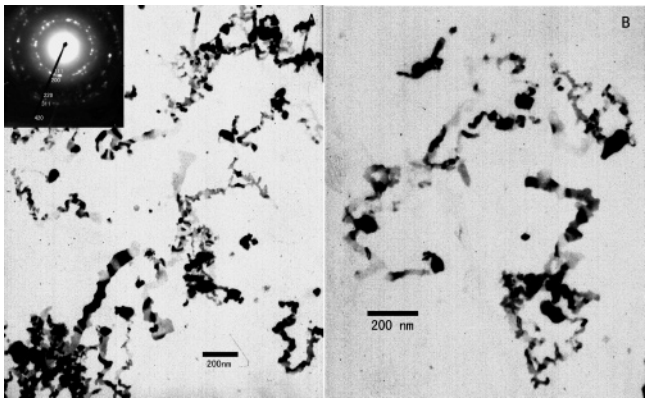


**Figure 5.** (A) Representative TEM image of gold nanoparticles produced by CFE at $5 \times 10^{-4}$ M $HAuCl_4$. Inset is the SAED pattern from gold nanoparticles corresponding to A. (B) Higher magnification TEM image of nanowires

longitudinal SPR absorption of the nanowires with different aspect ratios (*7*, *25*).

The corresponding TEM (Figure 5A and B) observations show the formation of gold nanowires with networked structure. This network structure is rigid enough to survive ultrasonic vibration in water after high-speed centrifugation. The diameter of the gold nanowires is approximately 50−60 nm. The SAED pattern obtained from the same wire shows individual diffraction rings originating from the {111}, {200}, {220}, {311}, and {420} reflections of the gold lattice structure, respectively, which further confirms the polycrystalline nature of these wires.

The formation of nanowire shapes can be attributed to both the Ostwald ripening at the expense of small gold nanoparticles and to the deposition of newly formed metallic gold by the reduction of gold ions. At the higher concentration of $HAuCl_4$, the CFE that acted as reduction and capping agent was insufficient relative to gold ions. More $AuCl_4^-$ may lead to the aggregation of tiny nanoparticles that show a tendency to undergo fusion into wire-like structures. At the concentration of $4.0 \times 10^{-4}$ M $HAuCl_4$, the relative excess of $AuCl_4^-$ may lead to formation of nanowires; however, there was not a sufficient amount of $AuCl_4^-$ capping on the surface of the nanowires, which led to breakage of the nanowires and aggregation of more thermodynamically stable nanoparticles. The sufficiency of $AuCl_4^-$ ($5.0 \times 10^{-4}$ M) capped on the surface of the nanowires maintained their shapes. ICP analysis (Figure S2, Supporting information) identified that the gold ions were completely consumed at the concentration of $2.5 \times 10^{-4}$ M $AuCl_4^-$. However, when the $AuCl_4^-$ concentration was $5 \times 10^{-4}$ M, a certain amount of gold ions still remained at the end of the reaction. A possible growth process of gold nanowires with

**Scheme 1. Schematic Growth Mechanism of Gold Nanowires with Network Structure**

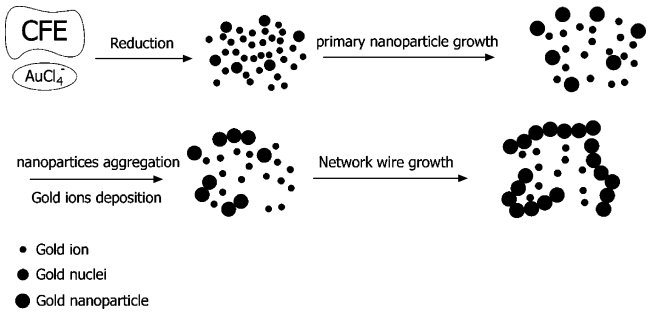


network structure is shown in Scheme 1, which includes the following stages. Gold ions are reduced to form gold nuclei by the CFE. The nuclei become nanoparticles by gathering reduced metallic gold surrounding the nuclei. The preliminarily formed gold nanoparticles are thermodynamically unstable in aqueous solution because of insufficient capping agent. At this point, they would tend to form linear assemblies driven by Brownian motion and short-range interaction and then the produced gold atoms deposit on the concave regions of the connected particles through capillary phenomenon, a located Ostwald ripening process, evolving into the networked nanostructures (*7*, *26*).

The mechanism of the reducing and shape-directing of gold nanoparticles is not elucidated clearly; the proteins that acted as reducing and capping agent in the CFE need thorough analysis including their purification, active biomolecules, sequence, and structure. All of this research needs extensive efforts. Our work is continuing to study the control of the shape, the size, and the biological mechanism of their formation.

## Conclusions

In conclusion, we developed a simple, room-temperature, and efficient biological method for synthesis of gold networked nanowires using CFE of the bacterium *R. capsulata*. It is probable that proteins acted as the major biomolecules involved in the bioreduction and synthesis of gold nanoparticles. It was shown that gold ions played an important role in forming and stabilizing the shape of gold nanowires. The gold nanowires had diameters between 50 and 60 nm. This method is expected to be applicable to the synthesis of other metallic nanowires such as silver and platinum. Even other anisotropic metal nanostructures are expected using the biosynthetic methods. The flexibility of gold nanowires that could be tuned could find applications in microelectronics, optoelectronics, nanoscale electronic devices, and other fields.

## Acknowledgment

The authors are grateful for financial support from NSFC, China (nos. 20573019, 60371027, 60171005, and 90406023) and National High-Tech 863 Program. We also thank Mr. Aiqun Xu from the Analysis and Testing Center of SEU for the TEM characterization.

**Supporting Information Available:** Supplementary TEM images of gold nanostructures synthesized at the $3.0 \times 10^{-4}$ M and $4.0 \times 10^{-4}$ M $AuCl_4^-$ concentration (S1) and figures showing the changes of $AuCl_4^-$ concentration (S2). This material is available free of charge via the Internet at http://pubs.acs.org.

## References and Notes

(1) Alivisatos, A. P. Perspectives on the physical chemistry of semiconductor nanocrystals. *J. Phys. Chem*. **1996**, *100*, 13226−13239.

(2) Jin, R.; Cao, Y.; Mirkin, C. A.; Kelly, K. L.; Schatz, G. C.; Zheng, J. G. Photoinduced conversion of silver nanospheres to nanoprisms. *Science* **2001**, *294*, 1901−1903.

(3) Aizpurua, J.; Hanarp, P.; Sutherland, D. S.; Kall, M.; Bryant, G. W.; Abajo, F. J. G. de. Optical properties of gold nanorings. *Phy. Rev. Lett*. **2003**, *90*, 057401-1−057401-4.

(4) Gao, J.; Bender, C. M.; Murphy, C. J. Dependence of the gold nanorod aspect ratio on the nature of the directing surfactant in aqueous solution. *Langmuir* **2003**, *19*, 9065−9070.

(5) Sun, Y.; Xia, Y. Shape-controlled synthesis of gold and silver nanoparticles. *Science* **2002**, *298*, 2176−2179.

(6) Murphy, C. J.; Gole, A. M.; Hunyadi, S. E.; Orendorff, C. J. One-dimensional colloidal gold and silver nanostructures. *Inorg. Chem.* **2006**, *45*, 7544−7554.

(7) Pei, L. H.; Mori, K.; Adachi, M. Formation process of two-dimensional networked gold nanowires by citrate reduction of $AuCl_4^-$ and the shape stabilization. *Langmuir* **2004**, *20*, 7837−7843.

(8) Wang, T.; Zhang, D.; Xu, W.; Li, S.; Zhu, D. New approach to the assembly of gold nanoparticles: formation of stable gold nanoparticle ensemble with chainlike structures by chemical oxidation in solution. *Langmuir* **2002**, *18*, 8655−8659.

(9) Li, Z.; Liu, Z.; Zhang, J.; Han, B.; Du, J.; Gao, Y.; Jiang, T. Synthesis of single-crystal gold nanosheets of large size in ionic liquids. *J. Phys. Chem. B* **2005**, *109*, 14445−14448.

(10) Sun, Y.; Mayers, B.; Xia, Y. Transformation of silver nanospheres into nanobelts and triangular nanoplates through a thermal process. *Nano Lett.* **2003**, *3*, 675−679.

(11) Hu, J.; Zhang, Y.; Liu, B.; Liu, J.; Zhou, H.; Xu, Y.; Jiang, Y.; Yang, Z.; Tian, Z. Synthesis and properties of tadpole-shaped gold nanoparticles. *J. Am. Chem. Soc*. **2004**, *126*, 9470−9471.

(12) Mandal, D.; Bolander, M. E.; Mukhopadhyay, D.; Sarkar, G.; Mukherjee, P. The use of microorganisms for the formation of metal nanoparticles and their application. *Appl. Microbiol. Biotechnol*. **2005**, *69*, 485−492.

(13) Beveridge, T. J.; Murray, R. G. E. Site of metal deposition in the cell wall of *Bacillus subtilis*. *J. Bacteriol*. **1980**, *141*, 876−887.

(14) Mukherjee, P.; Ahmad, A.; Mandal, M.; Senapati, S.; Sainkar, S. R.; Khan, M. I.; Ramani, R.; Parischa, R.; Ajayakumar, P. V. Bioreduction of $AuCl_4^-$ ions by the fungus, *Verticillium* sp. and surface trapping of the gold nanoparticles formed. *Angew. Chem., Int. Ed.* **2001**, *40*, 3585−3588.

(15) Ahmad, A.; Senapati, S.; Khan, M. I; Ramani, R.; Srinivas, V.; Sastry, M. Intracellular synthesis of gold nanoparticles by a novel alkalotolerant actinomycete *Rhodococcus* species. *Nanotechnology* **2003**, *14*, 824−828.

(16) Mukherjee, P.; Senapati, S.; Ahmad, A.; Khan, M. I.; Sastry, M. Extracellular synthesis of gold nanoparticles by the fungus *Fusarium oxysporum*. *ChemBiochem* **2002**, *3*, 461−463.

(17) Ahmad, A.; Senapati, S.; Khan, M. I.; Kumar, R.; Sastry, M. Extracellular biosynthesis of monodisperse gold nanoparticles by a novel extremophilic actinomycete, *Thermomonospora* sp. *Langmuir* **2003**, *19*, 3550−3553.

(18) Shankar, S. S.; Rai, A.; Ankamwar, B.; Singh, A.; Ahmad, A.; Sastry, M. Biological synthesis of triangular gold nanoprisms. *Nat. Mater.* **2004**, *3*, 482−488.

(19) Chandran, S. P.; Chauhary, M.; Pasricha, R.; Ahmad, A.; Sastry, M. Synthesis of gold nanotriangles and silver nanoparticles using *aloe vera* plant extract. *Biotechnol. Prog*. **2006**, *22*, 577−583.

(20) Xie, J. P.; Lee, J. Y.; Wang, D. L. C.; Ting, T. P. Identification of active biomolecules in the high yield synthesis of single-crystalline gold nanoplates in the alga solutions. *Small* **2007**, *4*, 672−682.

(21) He, S. Y.; Guo, Z. R.; Zhang, Y.; Zhang, S.; Wang, J.; Gu, N. Biosynthesis of gold nanoparticles using the bacteria *Rhodopseudomonas capsulata*. *Mater. Lett*. **2007**, *61*, 3984−3987.

(22) Gardea-Torresdey, J. L.; Parson, J. G.; Gomea, E.; Peraltaviden, J. R.; Troiani, H. E.; Santiago, P.; Yacaman, M. J. Formation and growth of Au nanoparticles inside live alfalfa plants. *Nano Lett.* **2002**, *2*, 397−401.

(23) Caruso, F.; Furlong, D. N.; Ariga, K.; Ichinose, I.; Kunitake, T. Characterization of polyelectrolyte-protein multilayer films by atomic force microscopy, scanning electron microscopy, and Fourier

transform infrared reflection-absorption spectroscopy. *Langmuir* **1998**, *14*, 4559−4565.
(24) Gole, A.; Dash, C.; Ramarkrishnan, V.; Sainkar, S. R.; Mandale, A. B.; Rao, M.; Sastry, M. Pepsin-gold colloid conjugates: preparation, characterization, and enzymatic activity. *Langmuir* **2001**, *17*, 1674−1679.
(25) Chen, C.; Yeh, Y.; Wang, C. R. C. The fabrication and photo-induced melting of networked gold nanostructures and twisted gold nanorods. *J. Phys. Chem. Solids* **2001**, *62*, 1587−1612.
(26) Yuan, J.; Wang, Z.; Zhang, Q.; Han, D.; Zhang, Y.; Shen, Y.; Niu, L. Controlled synthesis of 2D Au nanostructure assembly with the assistance of sulfonated polyaniline nanotubes. *Nanotechnology* **2006**, *17*, 2641−2648.

Received September 14, 2007. Accepted January 14, 2008.

BP0703174